

Quantitative Kinetic Model of CO₂ Absorption in Aqueous Tertiary Amine Solvents

Xavier Rozanska, Erich Wimmer, and Frédéric de Meyer*



Cite This: *J. Chem. Inf. Model.* 2021, 61, 1814–1824



Read Online

ACCESS |

Metrics & More

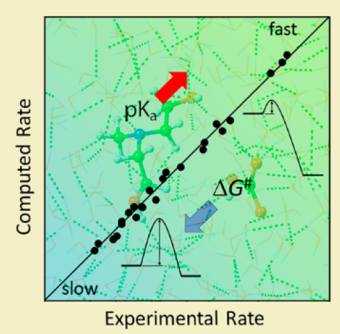
Article Recommendations

Supporting Information

ABSTRACT: Aqueous tertiary amine solutions are increasingly used in industrial CO₂ capture operations because they are more energy-efficient than primary or secondary amines and demonstrate higher CO₂ absorption capacity. Yet, tertiary amine solutions have a significant drawback in that they tend to have lower CO₂ absorption rates. To identify tertiary amines that absorb CO₂ faster, it would be efficacious to have a quantitative and predictive model of the rate-controlling processes. Despite numerous attempts to date, this goal has been elusive. The present computational approach achieves this goal by focusing on the reaction of CO₂ with OH⁻ forming HCO₃⁻. The performance of the resulting model is demonstrated for a consistent experimental data set of the absorption rates of CO₂ for 24 different aqueous tertiary amine solvents. The key to the new model's success is the manner in which the free energy barrier for the reaction of CO₂ with OH⁻ is evaluated from the differences among the solvation free energies of CO₂, OH⁻, and HCO₃⁻, while the pK_a of the amines controls the concentration of OH⁻. These solvation energies are obtained from molecular dynamics simulations. The experimental value of the free energy of reaction of CO₂ with pure water is combined with information about measured rates of absorption of CO₂ in an aqueous amine solvent in order to calibrate the absorption rate model. This model achieves a relative accuracy better than 0.1 kJ mol⁻¹ for the free energies of activation for CO₂ absorption in aqueous amine solutions and 0.07 g L⁻¹ min⁻¹ for the absorption rate of CO₂. Such high accuracies are necessary to predict the correct experimental ranking of CO₂ absorption rates, thus providing a quantitative approach of practical interest.

Rate of CO₂ Absorption

$r_{\text{abs}}(\text{CO}_2) \sim [\text{CO}_2][\text{OH}^-] e^{-\Delta G^\# / RT}$
 $[\text{OH}^-] \sim \text{pK}_a (\text{amine})$
 $\text{CO}_2 + \text{OH}^- \xrightarrow{\Delta G^\#} \text{HCO}_3^-$
 $\Delta G^\# \text{ depends on solvation}$
 $\text{of CO}_2, \text{OH}^-, \text{and HCO}_3^-$



1. INTRODUCTION

To capture CO₂ from flue gases or natural gas, the cyclic absorption/regeneration process based on aqueous primary or secondary amines is the most mature in industrial applications. Commonly used primary and secondary amines are monoethanolamine (MEA) and diethanolamine (DEA). These amines are relatively stable chemically, have low volatility, and are relatively noncorrosive. They possess ample net cyclic CO₂ absorption capacity and have a rapid reaction rate with CO₂. The main drawback of amine-based regeneration technology is the elevated regeneration energy required to heat the charged amine solvent to provide the energy for the desorption reaction. This necessary process heat produces steam to strip the CO₂ away from the solvent and make the desorption of CO₂ thermodynamically favorable.¹ The activation energy for this desorption reaction is relatively large, because unhindered primary and secondary amines form generally stable carbamates (R₂NCOO⁻) when reacting with CO₂. Carbamate formation follows the chemical reaction CO_{2(aq)} + 2R₂NH \rightleftharpoons R₂NCOO⁻ + R₂NH₂⁺. Depending on the stability of the carbamates formed, bicarbonate is also formed through the reaction R₂NCOO⁻ + H₂O \rightleftharpoons HCO₃⁻ + R₂NH.² In the presence of aqueous tertiary alkanolamines like *n*-

methyldiethanolamine (MDEA), CO₂ is only and directly bound as bicarbonate (HCO₃⁻) through the reaction CO_{2(aq)} + H₂O + R₃N \rightleftharpoons R₃NH⁺ + HCO₃⁻.³ Bicarbonate is nonvolatile and stable in water.

The heat of reaction for direct bicarbonate formation is much smaller than that for carbamate formation.^{2–4} This fact results in regeneration energy savings when only tertiary amines are used because they do not form carbamate. Moreover, the CO₂ absorption capacity is generally much greater as only one tertiary amine is required to convert one molecule of CO₂ into bicarbonate, while two molecules of primary or secondary amines are required to form a carbamate ion. Therefore, tertiary amines are increasingly used in industry to capture CO₂ from flue or natural gas. However, in general, the rate of direct bicarbonate formation is much lower than

Received: December 1, 2020

Published: March 12, 2021



that of carbamate formation, resulting in slower CO₂ absorption rates with tertiary amines.⁴

A considerable research effort is thus ongoing to identify tertiary amines that combine a low heat of reaction with a high CO₂ absorption rate. Different groups measured the CO₂ absorption rates for a relatively large set of tertiary amines representing a wide range of different structural characteristics. The ultimate goal of these efforts is to identify a quantitative relationship between CO₂ absorption rates and the structural and chemical properties (e.g., pK_a) of amines.^{4–9} However, until now, no quantitative and predictive model with sufficient accuracy was available to establish such a relationship, most likely due to the subtlety of the free energy differences that determine the reaction rates. An accurate CO₂ absorption rate model would be of great value for identifying tertiary amines with higher CO₂ absorption rates. For completeness, it should be mentioned that other groups attempt to catalyze the CO₂ absorption reaction in the presence of tertiary amines by adding an enzyme.¹⁰ Such an approach is outside the scope of the present work.

In this work, we present a highly accurate quantitative and predictive model for the CO₂ absorption rate in aqueous tertiary alkanolamine solvents. The model is applicable for a wide range of amine concentrations and temperatures and in the presence of physical cosolvents. We develop and validate this model with the largest consistent experimental study available in the literature.⁴

CO₂ reacts in basic solutions.¹¹ Intuitively, one expects that the rate of CO₂ absorption correlates mainly with the basicity of the amine, *i.e.*, with the pK_a value of the amines. While there is some correlation between CO₂ absorption rates and pK_a values, it is not fully convincing and useful.^{4–9} When one considers the direct reaction of CO₂ with a tertiary amine such as MDEA, the formation of an HCO₃⁻ ion requires a reaction between three molecules, namely CO₂, an intermediate water molecule, and the amine. By computing the free energy of the reaction barrier, one would thus be able to predict the reactivity of various amine solutions. Experience shows that this approach does not yield the necessary accuracy given the present computational tools. This shortcoming is evident, for example, from the work of Leung et al.,¹² who used *ab initio* molecular dynamics to model the reaction of CO₂ with water. The two weaknesses of this approach are (i) the necessity to sample a very large configurational space to get an accurate description of solvation effects and (ii), more fundamentally, the intrinsic uncertainties in solving Schrödinger's equation using current quantum chemical methods. Furthermore, the use of kinetics solvation models such as those proposed in the literature^{5,13,14} does not achieve the accuracy needed in the present context. Importantly, the reaction of CO₂ with OH⁻ does not necessarily require a termolecular reaction involving the protonation of the amine. OH⁻ ions exist in aqueous amine solutions and can react directly with CO₂. This consideration led us to the approach described below.

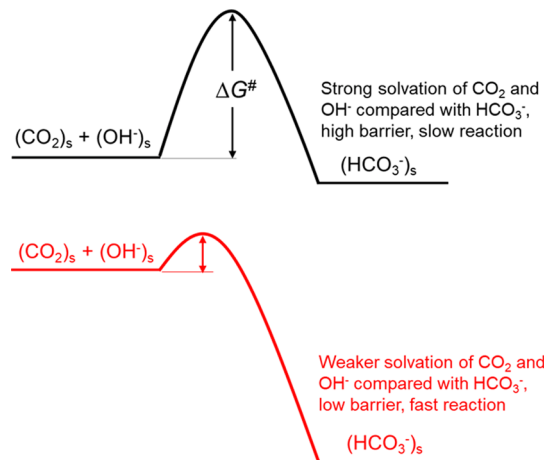
The present model assumes that (i) the concentrations of amine, protonated amine, H₃O⁺, and OH⁻ in an aqueous amine solvent are in equilibrium, (ii) the concentration of CO₂ depends on its partial pressure in the gas phase and its Henry constant, and (iii) the kinetics of CO₂ absorption is controlled by the reaction between solvated CO₂ and OH⁻ forming HCO₃⁻. Differences in the solvation of these three species due to the characteristics of each amine are critical. It turns out that this approach explains the experimental data when the

resulting equations are supplied with the relevant property values.

The concentrations of OH⁻ and CO₂ and the Gibbs free energy of activation of the reaction between CO₂ and OH⁻ are the values determining the reaction rate. The concentrations of solvated OH⁻ and CO₂ are obtained by solving the pH equation using as inputs the pK_a of the acid–base reactions in an aqueous amine solvent, the Henry constant of physical absorption of CO₂ in aqueous amine solvents, and the initial concentration of amine and pressure of CO₂. Atomistic simulations are used to quantify the Henry constants of CO₂ through the Gibbs free energies of solvation of CO₂.

The Gibbs free energy of activation of the reaction CO₂ + OH⁻ to HCO₃⁻ is obtained from the energies of solvation of each species using classical molecular dynamics and applying the Evans–Polanyi principle¹⁵ (Scheme 1) using experimental

Scheme 1. Evans–Polanyi Principle Links Linearly the Variation of an Activation Energy Barrier with Changes in the Solvation Energies of the Reactant and Product



data for pure water as calibration. This approach achieves high internal consistency and numerical stability, leading to an excellent agreement with the experimental reaction rates reported by Chowdhury et al.⁴ for 24 aqueous amine solutions.

2. METHODS AND COMPUTATIONAL DETAILS

This section describes the methods used to get each term in the expression of the rate of the absorption of CO₂

$$r_{\text{abs}} = a(T) \exp\left(-\frac{\Delta G^\ddagger}{RT}\right) [\text{CO}_2][\text{OH}^-] \quad (1)$$

where r_{abs} is the absorption rate to be compared with the experimental results by Chowdhury et al.,⁴ [CO₂] and [OH⁻] are the concentrations of carbon dioxide molecules and hydroxyl anions, respectively, ΔG^\ddagger is the Gibbs free energy barrier for the reaction CO₂ + OH⁻ to HCO₃⁻, RT is the macroscopic thermodynamic energy unit in which R is the universal gas constant, T is the absolute temperature, and $a(T)$ is a temperature-dependent pre-exponential factor.

2.1. Physisorption and Henry Constant of Solvation of CO₂. Quantum chemical Density Functional Theory (DFT) computations were done to obtain the Gibbs free energies of physisorption of CO₂ in aqueous amine solvents. The computed energy values were obtained using the Gaussian program¹⁶ as available in the MedeA software environment.¹⁷

Geometry optimization and frequency calculations were performed for all systems. The data from the frequency and energy calculations were used to get thermophysical and chemical properties.¹⁸ The DFT hybrid functional B3LYP^{19,20} was used with a 6-31G* basis set.^{21–23} The implicit solvation model (SMD) developed by Marenich et al.²⁴ was selected to predict Gibbs free energies of solvation.

Given the importance of solvation effects, there exists a wealth of options for implicit solvation methods besides the SMD approach. These methods are typically based on a polarizable dielectric embedding.²⁵ The Polarizable Continuous Model (PCM),^{26,27} the COnductor like Screening MOdel (COSMO),²⁸ the COnductor like Screening MOdel for Real Solvent (COSMO-RS),^{29,30} the three-dimensional reference interaction site model (3DRISM),^{31,32} and the harmonic solvation model³³ are prominent approaches among others. The advantages and drawbacks of implicit solvation methods have been analyzed in detail and reported in review articles (ref 34 and references therein). These reviews point out that one of the most critical drawbacks of implicit solvation methods is the challenge to describe the strong local hydrogen bonds and the difficulties to account for temperature dependent effects, in contrast to molecular dynamics simulations.³⁴ The issue of the hydrogen bonds is solved by explicit solvation methods or a hybrid explicit/implicit solvation protocol, where the first solvation shell around the solvated molecule is included explicitly while this cluster of molecules is embedded in a continuous dielectric environment.³⁴ The temperature dependent properties are dealt with when explicit dynamics simulations of the solute and solvent are performed.³⁴ On the other hand, implicit solvation models elegantly circumvent the problem of proper statistical sampling of the configurational space, which requires great care when using explicit molecular dynamics simulations. The choice of the most appropriate solvation approach depends on the system and the required accuracy. Thus, in the present work, we have adopted a hybrid strategy by using an implicit solvation model to obtain the solvation energy of molecular CO₂ while the solvation effects related to the reaction involving ionic species, namely OH[−] and HCO₃[−], are treated explicitly by molecular dynamics simulations, albeit that these simulations require significant computational effort. In the case of the physical solvation of a neutral CO₂ molecule, no strong hydrogen bonds are formed with its environment due to the high symmetry and apolar nature of this molecule.

The SMD approach belongs to the most recent generation of implicit solvation models.²⁴ Although it implicitly considers the solvent, it also explicitly takes into account additional properties and characteristics of the solvent such as the surface tension between the solute cavity and the solvent shell. Another attractive feature of the SMD approach is the fact that it uses the full electronic density of the solute. The merits, pitfalls, and approximations of the SMD method are described in ref 24. The SMD approach has been compared with other implicit solvation methods and was found to perform better or equivalently than PCM and COSMO for neutral molecules.²⁴ We found that the RMSD between the computed and experimental Gibbs free energy of physisorption of CO₂ obtained using the SMD method is 6.7 kJ mol^{−1} for a set of 75 physical solvents (Supporting Information), which is close to the reported accuracy of 4.2 kJ mol^{−1} of the SMD approach for 2346 absorption values of neutral molecules.²⁴ We empirically improved this accuracy to 1.3 kJ mol^{−1} for CO₂

to further reduce the error associated with the concentration of solvated CO₂ in the aqueous amine solvents in our estimation of the rate of absorption of CO₂ (Supporting Information). Notwithstanding the present choice of the SMD method, it is expected that the other approaches mentioned above are equally applicable to get the Gibbs free energy of solvation of CO₂.^{24–34}

To characterize a solvent in the SMD approach, seven specific properties of this solvent are required: the dielectric constant (ϵ), the polarizability, through the square of the solvent refractive index at 20 °C (n^2), the acidity and basicity Abraham's indices (α and β , respectively),^{35–37} the solvent surface tension (γ), the aromaticity, *i.e.*, the fraction of aromatic atoms per non-hydrogen atoms (Φ), and the halogenicity, *i.e.*, the fraction of halogen atoms per non-hydrogen atoms (Ψ). Φ and Ψ are equal to zero because there are no aromatic or halogen atoms in the solvents considered in this study. The five other parameters are common fluid properties accessible for many chemical compounds in databases from the literature.^{24,38,39} However, most of the 24 amines considered in this study are not available in experimental databases. To fill these gaps, we fitted Quantitative Structure–Property Relationship (QSPR)^{40,41} parameters using the group contribution descriptors of Joback and Reid.⁴² Details about this QSPR fitting, its parameters, and accuracy are found in the Supporting Information. Aqueous amine solvents are mixtures of water and amine. Mixing rules exist to derive fluid properties of mixtures from the pure fluids.^{43,44} For the sake of simplicity, we used the simplest relationship, in which the properties of the mixtures are that of the pure fluids weighted with respect to their mole fractions. In the case of the dielectric constant, this approximate procedure leads to an average error of 5%.⁴⁴ As mentioned, we improved the accuracy of the Gibbs free energies of physisorption of CO₂ to 1.3 kJ mol^{−1} (Supporting Information). We used this approach to correct our DFT Gibbs free energy values of solvation of CO₂. These values are used in the calculations of the pH values of aqueous amine solvents in the presence of gaseous CO₂ at low pressure. The root-mean-square deviation (RMSD) between the computed Gibbs free energy of absorption of CO₂ and the experimental data is 1.4 kJ mol^{−1} for a set of 59 solvents when using our QSPR method to provide the data for the SMD calculations (Supporting Information). Note that in this approach no experimental data for specific systems of interest are needed.

2.2. Concentrations of CO₂ and OH[−]. The concentrations of OH[−] and CO₂ are obtained by solving the pH equation for the systems under the initial conditions of concentration as given by Chowdhury et al.⁴ (30%w amine) and using the experimental pK_a of the amines (Tables 1 and 2), the pK_a values of H₂CO₃ and HCO₃[−], and the pK_E of water. Details of these calculations are provided in the Supporting Information, together with a comparison between our predictions and literature data for the case of aqueous MDEA.⁴⁵ In Table 2, we also include the experimental rates of CO₂ in the aqueous amine solvents.

2.3. Solvation Energies of CO₂, OH[−], and HCO₃[−]. The total energies of the aqueous amine solvents, with and without solvated CO₂, OH[−], and HCO₃[−], were evaluated by classical molecular mechanics (MM) dynamics simulations⁴⁶ using the Large-scale Atomic/Molecular Massively Parallel Simulator software (LAMMPS)⁴⁷ with the Extended Polymer Consistent Force Field (PCFF+)^{48–51} as implemented in MedeA 3.1.¹⁷

Table 1. List of Amines^a

amine label, name, and (abbreviation)	
1. 2-(dimethylamino)ethanol (DMAE)	13. <i>N</i> - <i>tert</i> -butyldiethanolamine (tBDEA)
2. 3-dimethylamino-1-propanol (DMA-1P)	14. 3-(dimethylamino)-1,2-propanediol (DMA-12-PD)
3. 2-diethylaminoethanol (DEAE)	15. 3-diethylamino-1,2-propanediol (DEA-12-PD)
4. 3-diethylamino-1-propanol (DEA-1P)	16. triethanolamine (TEA)
5. 1-dimethylamino-2-propanol (DMA-2P)	17. 1-(2-hydroxyethyl)pyrrolidine (1(2HE)PRLD)
6. 1-diethylamino-2-propanol (DEA-2P)	18. 3-pyrrolidino-1,2-propanediol (PRLD-12-PD)
7. 2-(diisopropylamino)ethanol (DIPAE)	19. 1-(2-hydroxyethyl)piperidine (1(2HE)PP)
8. 2-(dimethylamino)-2-methyl-1-propanol (DMA-2M-1P)	20. 3-piperidino-1,2-propanediol (3PP-12-PD)
9. 3-dimethylamino-2,2-dimethyl-1-propanol (DMA-22-DM-1P)	21. 1-methyl-2-piperidineethanol (1M-2PPE)
10. 4-ethylmethylamino-2-butanol (4EMA-2B)	22. 3-hydroxy-1-methylpiperidine (3H-1MPP)
11. <i>N</i> -ethyldiethanolamine (EDEA)	23. 1-ethyl-3-hydroxypiperidine (1E-3HPP)
12. <i>N</i> -isopropyldiethanolamine (IPDEA)	24. <i>N</i> -methyldiethanolamine (MDEA)

^aThe amine labels, names, and abbreviations actually refer to the aqueous amine 30%w solvents.

Table 2. Computed Concentrations of Some of the Different Species in Aqueous Amine Solvents (30%w) in the Presence of CO_{2(g)}, and Experimental pK_a and CO₂ Absorption Rates

solvent	amine pK _a	absorption rate ^a	10 ⁴ × [OH ⁻] ^b	10 ⁸ × [CO ₂][OH ⁻] ^c
1. DMAE	9.49	1.70	8.3	1.03
2. DMA-1P	9.54	1.47	8.1	0.99
3. DEAE	10.01	2.49	10.5	1.24
4. DEA-1P	10.29	2.60	11.5	1.35
5. DMA-2P	9.67	2.24	9.4	1.03
6. DEA-2P	10.18	1.66	11.3	1.25
7. DIPAE	10.03	1.01	9.7	1.11
8. DMA-2M-1P	10.34	1.18	12.9	1.42
9. DMA-22-DM-1P	9.54	1.08	7.4	0.84
10. 4EMA-2B	9.82	1.37	8.7	1.04
11. EDEA	8.86	0.70	4.1	0.51
12. IPDEA	9.12	1.36	5.1	0.59
13. tBDEA	9.06	1.91	4.8	0.51
14. DMA-12-PD	9.14	1.28	5.8	0.64
15. DEA-12-PD	9.89	3.40	9.1	1.05
16. TEA	7.85	0.75	1.5	0.18
17. 1-(2HE)PRLD	9.86	2.41	9.8	1.21
18. PRLD-12-PD	9.64	1.25	7.8	0.89
19. 1-(2HE)PP	9.76	2.22	8.8	1.01
20. 3PP-12-PD	9.49	3.33	6.6	0.75
21. 1M-2PPE	9.89	3.17	9.3	1.03
22. 3H-1MPP	8.94	1.08	5.0	0.56
23. 1E-3HPP	9.21	0.96	5.8	0.67
24. MDEA	8.65	1.56	3.7	0.43

^aIn g CO₂ L⁻¹ min⁻¹. ^bIn mol L⁻¹. ^cIn mol² L⁻². The gas pressure of CO₂ was held constant at 10 Pa.

The nonbonded energy terms were evaluated within a cutoff distance of 9.5 Å. Beyond the cutoff distance, the particle–particle–particle–mesh (PPPM)⁵² method was used for the Coulomb interactions, while a tail correction is applied for the van der Waals interactions.⁵³ Temperature and pressure were controlled using the Nosé–Hoover thermostat⁵⁴ and barostat,⁴⁶ respectively. The time step for the integration of the Newtonian equation of motion⁵⁵ was set to 0.25 fs. The compositions of the atomistic models of the aqueous amine solvents in the MM simulations reflect the experimental ones (*Supporting Information*). The initial configurations, with imposed periodic boundary conditions and a density set to 0.7 g L⁻¹, were generated using the Amorphous Materials Builder module,¹⁷ which employs a Monte Carlo approach sampling the translational, rotational, and conformational degrees of freedom of component species to generate realistic config-

urations of atomistic models. Once the models were generated, they were equilibrated at T = 363 K for 1.5 ns of simulation in the isothermal-isochoric (NVT) ensemble before equilibration in the isothermal-isobaric (NPT) ensemble at P = 1 atm with a fluctuating temperature from 363 to 313.15 K for 1 ns. Next, the systems were further relaxed for 0.5 ns in the NPT ensemble at P = 1 atm and T = 313.15 K. Following this equilibration procedure, an NPT simulation at P = 1 atm and T = 313.15 K for 5 ns was performed to determine the average density of each system. This computed average density is also used to determine the cell volume of each aqueous amine system and consequently the amine's concentration (*Supporting Information*).

Following the 5 ns molecular mechanics simulation in the NPT ensemble of each aqueous amine solvent, the final structure is collected and duplicated: in the first duplicated

system, OH^- and CO_2 are inserted in the cell, and in the second, HCO_3^- is added. OH^- , CO_2 , and HCO_3^- were placed in the cells so as to be surrounded with water molecules (Figure 1). The densities of the two systems are set to the

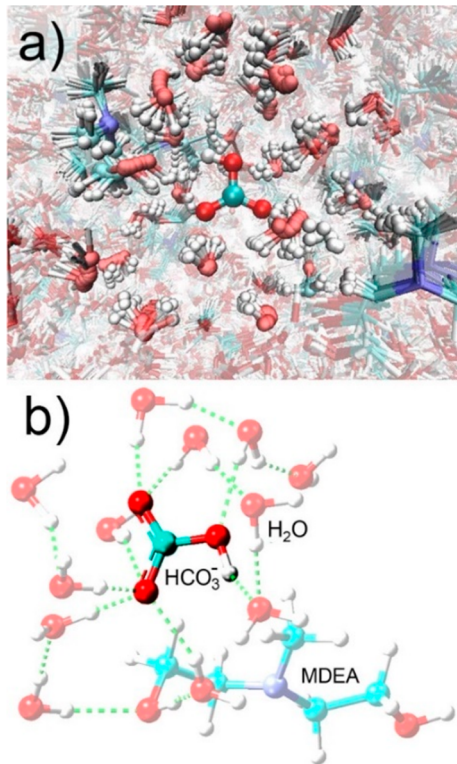


Figure 1. (a) Solvation of HCO_3^- in an aqueous solution of methyldiethanolamine (MDEA). The figure shows an overlay of 12 snapshots during about 1 ps of a molecular dynamics simulation at 313 K. For graphical clarity, the positions of the atoms in the bicarbonate anion are kept fixed. (b) View of a single snapshot of the first and second solvation shells around HCO_3^- in an aqueous MDEA solvent. The dashed lines indicate hydrogen bonds.

value obtained from the 5 ns NPT simulation of an aqueous amine solvent in the absence of OH^- and CO_2 or HCO_3^- . Because $\text{OH}^- + \text{CO}_2$ have the same mass as HCO_3^- , the volume of the aqueous amine, whether with $\text{OH}^- + \text{CO}_2$ or HCO_3^- periodic models, is identical. The total energies of the aqueous amine solvents, with and without solvated CO_2 , OH^- , and HCO_3^- , were evaluated from simulations in the NVT ensemble at $T = 313$ K. The energies were sampled over a series of runs. One and 3 ns runs were first performed followed by five batches of 5 ns NVT runs. The average final energies are the arithmetic simulated-time weighted averages. In some exceptional cases, extreme low or high energy values were discarded in the arithmetic average depending on their deviation with respect to the average, resulting in a minimum sampling time of 20 ns and up to a maximum of 29 ns. A value was considered extreme when its deviation was more than twice the standard deviation with respect to the average value.

2.4. Calibration. We computed the Gibbs free energies of activation using the solvation energies of CO_2 , OH^- , and HCO_3^- obtained from molecular dynamics simulations. The Evans–Polanyi principle,¹⁵ which is calibrated using experimental values for pure water and a training set of 10 aqueous amine solvents, namely 1–4, 7, 9, 11, 15, 16, and 24 (Table

1), was employed in deriving these values. As pointed out by Couchaux et al.,¹⁴ a renormalization of rates must be carried out when using experimental values from different sources. To avoid the ambiguities that remain associated with such renormalization, we confine the experimental data set to that used by Chowdhury et al.,⁴ since these data were obtained under the same conditions of temperature, amine concentration, initial pressure of CO_2 , and CO_2 production rates (Table 2). The amines discussed in Chowdhury et al.⁴ are representative of industrial solvents in CO_2 absorption processes.

The computed differences of free energy of absorption for HCO_3^- and $[\text{CO}_2 + \text{OH}^-]$ obtained from the molecular dynamics simulations are reported in Table 3. Note that each value in this table is obtained from two sets of molecular dynamics runs and hence corresponds to sampling times between 40 and 58 ns.

Table 3. Difference of Free Energy of Solvation of HCO_3^- and $\text{CO}_2 + \text{OH}^-$ in a 30%w Aqueous Amine Solvent^a

amine	ΔG	amine	ΔG
1. DMAE	-97.0	13. tBDEA	-101.0
2. DMA-1P	-96.0	14. DMA-12-PD	-96.2
3. DEAE	-98.1	15. DEA-12-PD	-102.0
4. DEA-1P	-98.0	16. TEA	-98.2
5. DMA-2P	-98.7	17. 1-(2HE)PRLD	-98.6
6. DEA-2P	-95.4	18. PRLD-12-PD	-95.4
7. DIPAE	-91.2	19. 1-(2HE)PP	-98.4
8. DMA-2M-1P	-92.1	20. 3PP-12-PD	-103.7
9. DMA-22-DM-1P	-94.4	21. 1M-2PPE	-101.5
10. 4EMA-2B	-94.4	22. 3H-1MPP	-96.2
11. EDEA	-93.3	23. 1E-3HPP	-93.6
12. IPDEA	-97.6	24. MDEA	-99.6

^aIn kJ mol^{-1} . The values are obtained from the molecular dynamics simulations.

ΔG in Table 3 is not the Gibbs free energy of activation of the reaction $\text{OH}^- + \text{CO}_2 \rightarrow \text{HCO}_3^-$ itself, but it can be related to ΔG^\ddagger by applying the Evans–Polanyi relationship:^{15,56}

$$\Delta G^\ddagger = a\Delta G + b \quad (2)$$

To further reduce the degrees of freedom in optimizing a and b in eq 2, we used the experimental value of the $\text{OH}^- + \text{CO}_2$ reaction at infinite dilution in aqueous NaOH solution, which is $50.62 \text{ kJ mol}^{-1}$.¹¹ We computed ΔG using the same molecular mechanics protocol as in the case of the aqueous amine for a pure water system. The model in the MM simulations consisted of 250 water molecules and $\text{OH}^- + \text{CO}_2$ or HCO_3^- . ΔG was found to be $-90.5 \text{ kJ mol}^{-1}$. The value for a was optimized to minimize the RMSD between the experimental reaction rates and the rates computed according to eq 2 for the 10 solvents as mentioned above. Subsequently, b in eq 2 is set such that ΔG^\ddagger in the case of the pure water system is the same as the experimental value of $50.62 \text{ kJ mol}^{-1}$. We obtained $a = 0.329$ and $b = 80.410 \text{ kJ mol}^{-1}$. The Gibbs free energies of activation are reported in the Supporting Information. To further develop a model that represents eq 1, we used

$$r_{AB,\text{model}} = A \exp\left(-\frac{a\Delta G + b}{RT}\right)([\text{OH}^-][\text{CO}_2] + B) \quad (3)$$

and optimized A and B to minimize the RMSD between the experimental and computed rates. A contains $\frac{k_{\text{BT}}}{h}$ and also a term to convert the unit from $\text{mol L}^{-1} \text{s}^{-1}$ to $\text{g of CO}_2 \text{ per L of solvent per min}$ ($\text{g L}^{-1} \text{ min}^{-1}$). This unit conversion puts A in the same units in which the experimental rates of Chowdhury et al.⁴ are expressed. Furthermore, the experimental rates of Chowdhury et al.⁴ were obtained by measuring the rate at 50% toward the completion of the reaction, which was assumed occurring in 60 min. This explains why the $[\text{OH}^-][\text{CO}_2]$ values in Table 2, which are representative of an initial concentration condition, need to be recalibrated by B . We found $A = 1.611 \times 10^{16} \text{ g CO}_2 \text{ min}^{-1} \text{ L mol}^{-2}$ and $B = 3.490 \times 10^{-9} \text{ mol}^2 \text{ L}^{-2}$. We used the 10 training solvents among the 24 as mentioned above to determine the parameters A and B . This amounts to a calibration of the model to specific experimental conditions. The RMSD between the rates computed using eq 3 and the experimental rates is $83 \text{ mg L}^{-1} \text{ min}^{-1}$. The RMSD on the validation set of 14 amines is $62 \text{ mg L}^{-1} \text{ min}^{-1}$. When the equation is applied to all 24 amines, we find an RMSD of $72 \text{ mg L}^{-1} \text{ min}^{-1}$. Randomly selecting training sets of 10 different solvents for this calibration has almost no influence on the values of A and B in eq 3, and the RMSD remains $72 \text{ mg L}^{-1} \text{ min}^{-1}$ (Supporting Information). The experimental and computed CO_2 absorption rates are reported in Figure 2 and in the Supporting Information. The corresponding structures of the amines are shown in Figure 3.

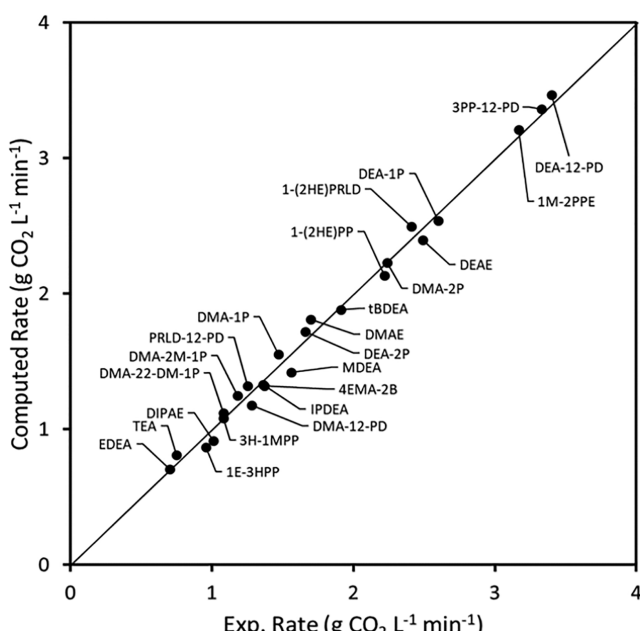


Figure 2. Experimental and computed rates of absorption of CO_2 in aqueous amine solvents (30%w) at 313 K. Source of experimental data: Chowdhury et al.⁴

3. DISCUSSION

While it would be desirable to have a model that can accurately predict CO_2 absorption rates for any solvent and any reaction at any concentration and temperature and for any experimental setup, the entire process of CO_2 absorption involves such a large number of factors at many length and time scales and it is so subtle, that such an endeavor would be too unwieldy. The present model focuses on a critical rate-limiting aspect, namely,

ΔG^\ddagger , the Gibbs free energy of activation of the reaction of CO_2 molecules with OH^- ions dissolved in an aqueous tertiary amine solvent, which appears to be the key aspect in the determination of the rate of absorption of CO_2 in this solvent. In addition to ΔG^\ddagger , the concentrations of dissolved CO_2 and of the OH^- ions are needed as well. All other aspects such as the geometry and dynamics of the gas/liquid interface, various diffusion processes, and other aspects of the experimental procedure are captured by three parameters for calibration.

We established a procedure for computing the rates of CO_2 absorption in aqueous amine solvents that relies primarily on the solvation properties of OH^- , CO_2 , and HCO_3^- obtained from atomistic simulations. The kinetic model that is used and its parameters and calibration have a clear and unambiguous interpretation (eq 3). The agreement achieved with experimental rates is excellent, with an RMSD = $0.07 \text{ g L}^{-1} \text{ min}^{-1}$ relative to the experimental data, which implies an accuracy of the calculated value for the Gibbs free energy of activation of 0.14 kJ mol^{-1} , assuming that there is no error in the values for the concentration of $[\text{OH}^-][\text{CO}_2]$ in eq 3, while the reported accuracy for the implicit solvation Gibbs free energy of ions is 17 kJ mol^{-1} with SMD.²⁴ The accuracy of the present approach is 1 order of magnitude better than what can be obtained using advanced high precision quantum chemical methods.^{57,58} This dramatically improved accuracy is made possible by a classical force field approach employing molecular dynamics simulations sampling times of the order of 50 ns for each value of the difference of the solvation energies of HCO_3^- , CO_2 , and OH^- . Here, the Evans–Polanyi relationship is used to estimate the Gibbs free energies of activation from the molecular dynamics free energies of solvation.^{15,56} The Evans–Polanyi relationship is calibrated on experimental data. Considering the impact of small changes of ΔG^\ddagger on the computed rates of absorption, it is judged that aggregating data either from different groups or different experimental measurement protocols would introduce unacceptable, uncontrolled errors into the fitting procedure. Couchaux et al.¹⁴ pointed out the need for caution and renormalization of experimental data of CO_2 absorption in aqueous amine solvents (concentration among others) when attempting to compare experimental data from different sources. Given that measured absorption rates depend on a number of experimental parameters, computational investigations have to be based on a consistent set of experimental data obtained with a given protocol. This is exemplified by the fact that the experimental data in Chowdhury et al. (refs 4 and 6) do not rank equally. For this reason, we focused exclusively on the data obtained by using the same apparatus under the same reaction conditions, with the A , B , and a parameters in our model containing information about this particular setup. Hence, these parameters need to be recalibrated for different experimental protocols. The model is valid as long as the rate of absorption of CO_2 is limited by the activation barrier of the reaction $\text{OH}^- + \text{CO}_2 \rightarrow \text{HCO}_3^-$ and the concentrations of OH^- and CO_2 . Note that the A and B parameters are independent of the activation barrier and the concentrations of OH^- and CO_2 . Hence, recalibration of the parameters A , B , and a would not require any additional demanding molecular dynamics simulations.

The model requires the Gibbs free energy of activation of the $\text{CO}_2 + \text{OH}^- \rightarrow \text{HCO}_3^-$ reaction in an aqueous tertiary amine solvent, the Gibbs free energy of absorption of CO_2 in this solvent, and the pK_a of the amine. The value of ΔG^\ddagger

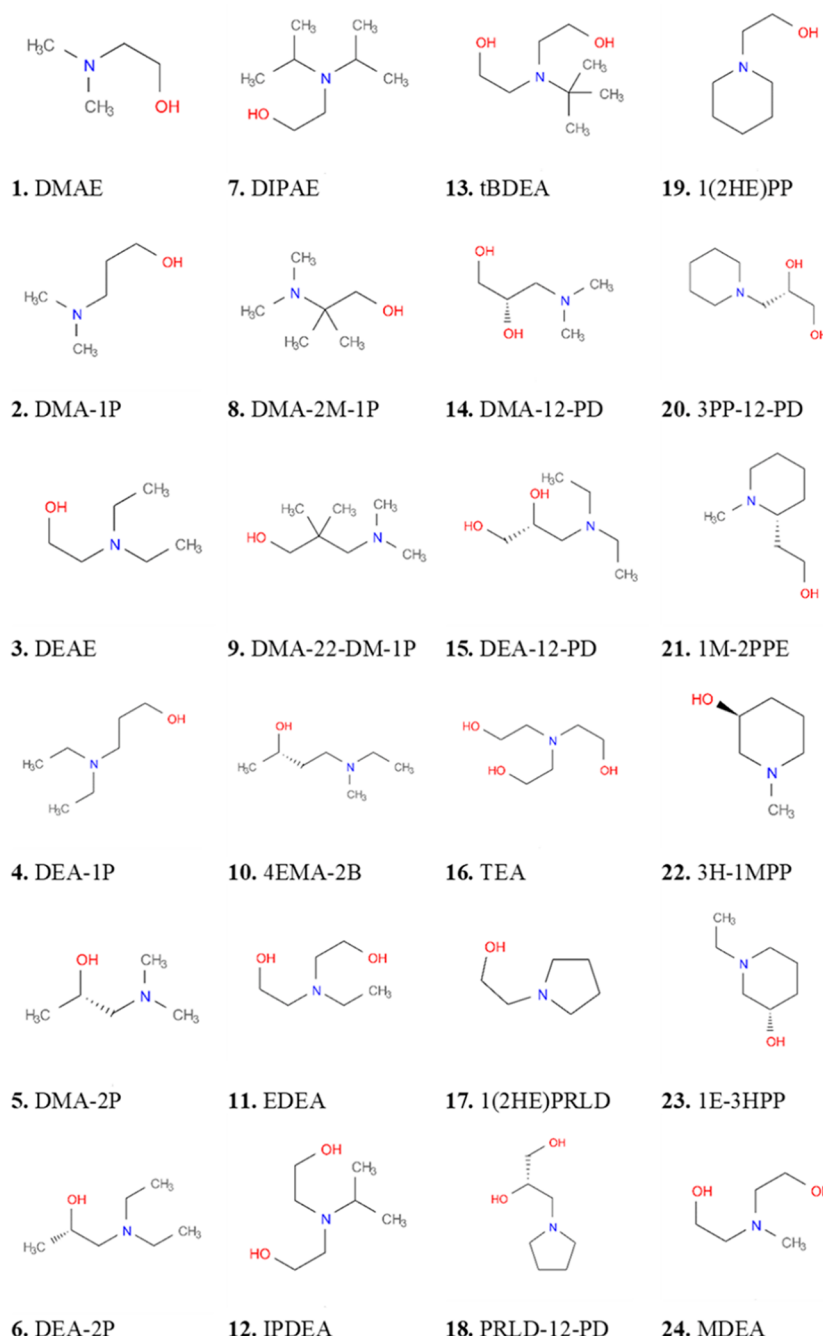


Figure 3. Structures of the 24 amines in the aqueous amine solvents investigated in this study.

demands a high accuracy because it contributes exponentially to the rate expression (eq 3). In the present work, we used experimental pK_a values of the amines.⁴ In case the pK_a values are not experimentally known, there exists a range of methods to compute them.^{41,59–62} The same applies to the determination of the Gibbs free energy of absorption of CO_2 ,^{63,64} which is needed to get $[\text{CO}_2]$. Any of the available computational methods can be used to determine the concentrations of CO_2 and OH^- .^{25–34,41,45,59–66} The resulting error on the rate of absorption of CO_2 will be linearly proportional to the error on the OH^- and CO_2 concentrations and, therefore, exponentially proportional to the error on the pK_a .^{65,66}

The predictive power of the present model is retained when computed pK_a values are used. The relative RMSDs between the computed and experimental rates on the 24 amines are 2.1% and 13.7% when the pK_a values are taken from experiments and QSPR,⁶⁰ respectively (Supporting Information). This QSPR method is characterized by an RMSD of 0.29 for the pK_a of the present 24 amines. Recently, Sakti et al.⁶² used an elaborated advanced quantum chemical explicit metadynamics simulation protocol to compute the pK_a of a set of 34 amines and found that the RMSD between the experimental and computed data was 0.09. In the absence of experimental pK_a data, this method would certainly be of great value to retain the overall predictive power of the present computational approach.

The model can be applied in screening studies of large number of systems. In this context, the simulations can be extended to other aqueous amines, concentrations, addition of a cosolvent, and different temperatures, which are input parameters in the molecular dynamics simulations, if these variations lead to conditions that remain close to those assumed in the current simulations, (e.g., $\Delta T = 10$ K or amine concentrations from approximately 5%mol to 13%mol). These limits should allow a similar qualitative and quantitative ranking of such other systems compared to those in Chowdhury et al.⁴

To test the range of applicability of the current model, we reprocessed the whole set of 24 aqueous amine solvents but at $T = 323$ K, with an initial amine concentration of 13%mol. This concentration was selected because it represents the maximum concentration that is industrially used in separation units. 13%mol ranges from 42.5%w for DMAE to 57.2%w for ^tBDEA. The computed rates of absorption of CO_2 at $T = 313$ and 323 K and 30%w and 13%mol aqueous amine solvents are reported in Figure 4. There is a factor of almost two difference

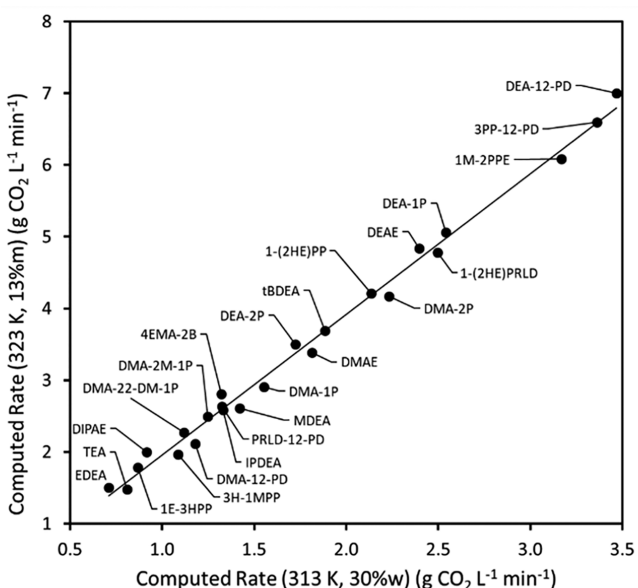


Figure 4. Computed rates of absorption of CO₂ in aqueous amine solvents at 313 K and 30%w and 323 K and 13%mol.

between the rates at 323 and 313 K, higher temperature rates being faster than those at lower temperature. This trend with temperature is consistent with [eqs 1](#) and [3](#) and an Arrhenius relationship. Few variations can be seen between the rates at different temperatures and concentration ([Figure 4](#)). These small variations are explained by changes in concentration when the amine concentrations are 30%w or 13%mol. The consistency of the computed rates of absorption in [Figure 4](#) is highlighted when only the computed activation energies are analyzed. The computed Gibbs free energies of activation at 313 and 323 K are reported in [Figure 5](#). These values can be related through the linear function:

$$\Delta G_{(323\text{K}, 13\%\text{mol})}^{\pm} = \Delta G_{(313\text{K}, 30\%\text{w})}^{\pm} + 0.34 \quad (4)$$

The standard deviation between the computed Gibbs free energies of activation at 323 K obtained from molecular dynamics simulations and those obtained using eq 4 is only

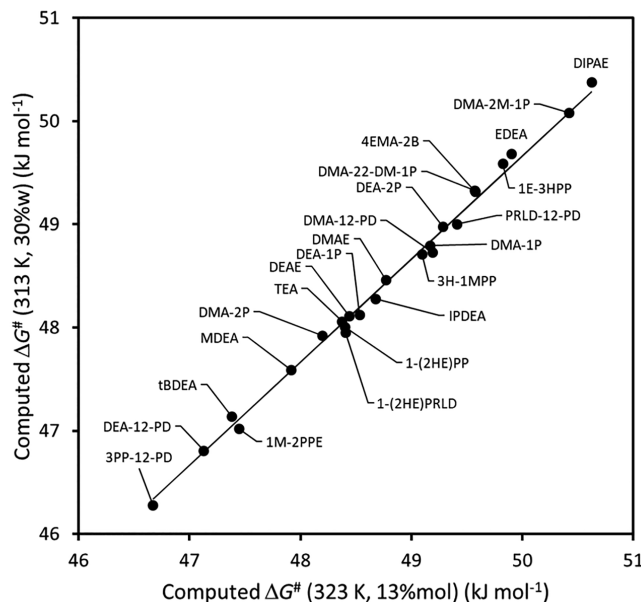


Figure 5. Computed Gibbs free energies of activation of absorption of CO₂ in aqueous amine solvents at 313 K and 30%w and 323 K and 13%mol.

0.07 kJ mol⁻¹. From eq 4, and assuming that the entropy variation associated with the amine concentration change can be neglected and that the entropy is unchanged with each amine, the entropy of activation is estimated to be -34 J mol⁻¹ K⁻¹ under these conditions, which is a typical value for CO₂ absorption in aqueous amine solvents.¹⁴

When the CO₂ absorption rates are plotted as a function of the Gibbs free energies of activation of the OH⁻ + CO₂ reaction (ΔG^\ddagger) and the concentration product [OH⁻][CO₂], one can better visualize the relationship between these quantities as they are related by eq 3 (Figure 6). As reported in previous studies,^{4,5,14} a relation between pK_a and CO₂ absorption rates indeed exists because of the [OH⁻] term (eq 3). The concentration of [OH⁻] varies with amine concentration and pK_a. The impact of amine concentration on [OH⁻] and the need for renormalization when considering rates from different sources were noted by Couchaux et al.¹⁴ Yet, additional quantities determine the CO₂ absorption rate in eq 3, namely [CO₂] and ΔG^\ddagger . [CO₂] is controlled by the Gibbs free energy of physisorption of CO₂ in the solvent and the gas pressure of CO₂. ΔG^\ddagger , which is not correlated with the pK_a of the amines (Supporting Information), is determined from the solvation energies of OH⁻, CO₂, and HCO₃⁻. Eq 3 explains why kinetic correlations based only on pK_a are unexpectedly weak.

Beyond simulation and computational models, the rationalization of the CO₂ absorption rate into clear and identified contributions is essential. The choice of amine plays an important role: it directly controls the CO₂ absorption rate through OH⁻ concentration and it affects ΔG[‡]. The amine also modifies the Henry constant of solvation of CO₂, which affects the rate of absorption as well. Finally, the amine changes ΔG[‡], which is 50.62 kJ mol⁻¹ in pure water and becomes 48.5 ± 1.5 kJ mol⁻¹ in the aqueous amine solvents investigated in the present work. However, we did not find a sufficiently accurate structure–activity relationship between ΔG[‡] and the structures of the amines to be quantitatively useful. The

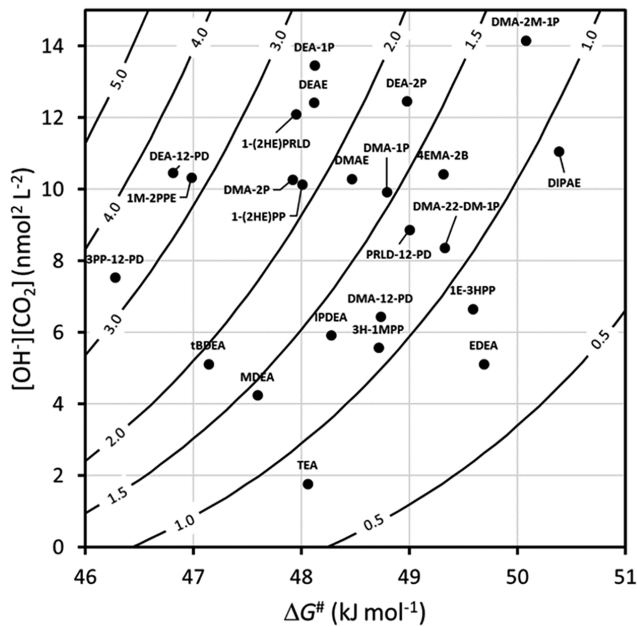


Figure 6. Nomograph of the rate of absorption of CO_2 at 313 K in 30%w aqueous amine solvents as a function of the computed Gibbs free energies of activation and $[\text{OH}^-][\text{CO}_2]$ concentrations. The lines are the iso-rate of absorption of CO_2 , where the values are in $\text{g CO}_2 \text{ L}^{-1} \text{ min}^{-1}$.

disruption of solvation by pure water leads to a lowering of the activation barrier of absorption of CO_2 in the aqueous amine solvents. In fact, the limit of no solvation is readily obtained from quantum chemical calculations of a CO_2 molecule interacting with an OH^- ion in vacuum. In this case, the barrier for the reaction $\text{CO}_2 + \text{OH}^- \rightarrow \text{HCO}_3^-$ vanishes. Thus, a comparison of the two extreme cases, namely, complete solvation in pure water and no solvation in vacuum, provides insight into the impact of amines on solvation due to cooperative multimolecular effects.

4. CONCLUSIONS

We established a quantitative and predictive procedure for computing the rates of CO_2 absorption in aqueous amine solvents. The extremely high accuracy required to achieve a meaningful ranking of different amines hinges on (i) the fact that the difference in the solvation energies of the reactants CO_2 and OH^- vs that for the product HCO_3^- plays a key role, and (ii) the absolute value of the free energy of CO_2 absorption can be calibrated based on the accurately known experimental value for $\text{CO}_2 + \text{OH}^- \rightarrow \text{HCO}_3^-$ Gibbs free energy of activation in pure water. Changes in solvation energies for different aqueous amine solvents can be computed with high numerical precision from molecular dynamics simulations using classical force fields. Amine molecules disrupt the solvation shells of the three solvated species due to complex, collective dynamical processes. These effects appear to be well captured by the present explicit molecular dynamics simulations, whereas the use of implicit solvation models and of quantitative structure–property relationships based on cheminformatics is extremely challenging because small changes in the amine structure combined with cooperative solvent effects have a strong impact on the absorption rates.^{67–72} This has also been reported in the

literature for other cases of reactions in solvated environments.^{73,74}

The present kinetic model, its parameters, and its calibration have a clear and unambiguous interpretation. The agreement of its predictions with experimental rates is excellent, with an RMSD of $0.07 \text{ g L}^{-1} \text{ min}^{-1}$ to the experimental data. Two main contributions explain the variation of the rates of absorption, namely (i) the concentration of the reactants and (ii) the Gibbs free energy of the activated complex. The fact that the absorption rate is proportional to the concentrations of OH^- and CO_2 supports the experimental observations that the amine's pK_a and rates of absorption of CO_2 are related (but not quantitatively correlated). The second term varies exponentially with the Gibbs free energy of activation of the reaction between $\text{OH}^- + \text{CO}_2$ in an aqueous amine solvent. This activation energy is found to change linearly with the solvation energies of OH^- and CO_2 and HCO_3^- following an Evans–Polanyi relationship. Accounting for both contributions is critical for achieving a quantitative model of CO_2 absorption.

The present model is valid as long as the rate of absorption of CO_2 is limited by the activation barrier of the reaction $\text{OH}^- + \text{CO}_2 \rightarrow \text{HCO}_3^-$ and the concentrations of OH^- and CO_2 . For example, the model would no longer be applicable when the ingress of CO_2 from the gas to liquid phases and/or the diffusion of CO_2 or OH^- are the rate limiting steps.

Once the model has been established for an experimental protocol, adapting it to other conditions and experimental protocols requires recalibration of only three parameters, namely A , B , and a (eq 3). The present work indicates that approximately ten experimental data points are sufficient for this calibration. To this end, no demanding additional molecular dynamics simulations would be needed. Application of the model to any other aqueous tertiary amine solvents requires the calculations of the difference of the solvation energies of $\text{CO}_2 + \text{OH}^-$ and of HCO_3^- in the new solvent, but no recalibration of the parameters is needed.

In summary, a quantitative model has been established for the prediction of absorption rates of CO_2 in aqueous amine solutions. The model offers a deep understanding of the subtleties of the controlling reaction mechanisms, in which solvation effects appear to play a critical role. Extensive molecular dynamics simulations, the Evans–Polanyi principle,¹⁵ and a calibration on experimental data for pure water as solvent are the key ingredients of this model. The present model achieves a level of accuracy that opens the door for efficient large-scale screening searches for optimized and novel solvents for the absorption of CO_2 , thus supporting the development of improved CO_2 absorption processes and a cleaner environment.

■ ASSOCIATED CONTENT

SI Supporting Information

The Supporting Information is available free of charge at <https://pubs.acs.org/doi/10.1021/acs.jcim.0c01386>.

Geometries and content of molecular dynamics models of aqueous amine solvents; details and explanation of analytical pH equation and speciation calculations; details, explanations, and parameters of QSPR method to get SMD parameters of amines; details and explanation to empirically correct implicit Gibbs free energy of solvation of CO_2 ; details and explanations of validation of computed Gibbs free energy of absorption

of CO₂; graph of Gibbs free energy of activation of absorption of CO₂ in aqueous amine solvents as function of pK_a of amine; graph of computed rate of absorption of CO₂ in aqueous amine solvents as function of pK_a of amine; table with computed Gibbs free energies of activation in aqueous amine solvents; table with details of computed and experimental rates of absorption of CO₂ in aqueous amine solvents; table with predicted fluid properties of amines; table with statistical analysis when different training sets are used to train parameters in equation of rate of absorption of CO₂; and table with QSPR pK_a and rates of absorption of CO₂ ([PDF](#))

AUTHOR INFORMATION

Corresponding Author

Frédéric de Meyer — TOTAL SE, Total Exploration Production, Liquefied Natural Gas — Acid Gas Entity, CCUS R&D Program, 92078 Paris, France; MINES ParisTech, PSL University, Centre de thermodynamique des procédés (CTP), 77300 Fontainebleau, France; [orcid.org/0000-0001-6717-1419](#); Email: frederick.de-meyer@total.com

Authors

Xavier Rozanska — Materials Design SARL, 92120 Montrouge, France

Erich Wimmer — Materials Design SARL, 92120 Montrouge, France

Complete contact information is available at:

<https://pubs.acs.org/10.1021/acs.jcim.0c01386>

Author Contributions

All authors have given approval to the final version of the manuscript.

Funding

This work was supported by the Carbon Capture Utilization and Storage R&D program from Total S.E. Exploration & Production.

Notes

The authors declare no competing financial interest.

ACKNOWLEDGMENTS

The authors gratefully thank Dr. Christophe Coquelet from MINES ParisTech, PSL University, Centre de thermodynamique des procédés, Dr. Clint Geller from Materials Design for the fruitful discussions and reviewing of this manuscript, Dr. Sukanta Kumar Dash for making his data available, and the entire team of Materials Design for their support. All calculations were performed with the computer resources of Materials Design.

REFERENCES

- (1) Kohl, A. L.; Nielsen, R. *Gas Purification*, 5th ed.; Gulf Professional Publishing: 1997.
- (2) Versteeg, G.; Van Swaaij, W. *Chem. Eng. Sci.* **1988**, *43*, 573–585.
- (3) Versteeg, G.; van Swaaij, W. *Chem. Eng. Sci.* **1988**, *43*, 587–591.
- (4) Chowdhury, F. A.; Yamada, H.; Higashii, T.; Goto, K.; Onoda, M. *Ind. Eng. Chem. Res.* **2013**, *52*, 8323–8331.
- (5) Puxty, G.; Rowland, R.; Allport, A.; Yang, Q.; Bown, M.; Burns, R.; Maeder, M.; Attalla, M. *Environ. Sci. Technol.* **2009**, *43*, 6427–6433.
- (6) Chowdhury, F. A.; Okabe, H.; Shimizu, S.; Onoda, M.; Fujioka, Y. *Energy Procedia* **2009**, *1*, 1241–1248.
- (7) Xiao, M.; Liu, H.; Idem, R.; Tontiwachwuthikul, P.; Liang, Z. *Appl. Energy* **2016**, *184*, 219–229.
- (8) Hartono, A.; Vevelstad, S. J.; Ciftja, A.; Knuutila, H. K. *Int. J. Greenhouse Gas Control* **2017**, *58*, 201–211.
- (9) Bernhardsen, I.; Knuutila, H. *Int. J. Greenhouse Gas Control* **2017**, *61*, 27–48.
- (10) Alvizo, O.; Nguyen, L. J.; Savile, C. K.; Bresson, J. A.; Lakhpatri, S. L.; Solis, E. O. P.; Fox, R. J.; Broering, J. M.; Benoit, M. R.; Zimmerman, S. A.; Novick, S. J.; Liang, J.; Lalonde, J. J. *Proc. Natl. Acad. Sci. U. S. A.* **2014**, *111*, 16436–16441.
- (11) Pinsent, B. R. W.; Pearson, L.; Roughton, F. J. W. *Trans. Faraday Soc.* **1956**, *52*, 1512–1520.
- (12) Leung, K.; Nielsen, I. M.; Kurtz, I. *J. Phys. Chem. B* **2007**, *111*, 4453–4459.
- (13) Carey, T. R.; Hermes, J. E.; Rochelle, G. T. *Gas Sep. Purif.* **1991**, *5*, 95–109.
- (14) Couchaux, G.; Barth, D.; Jacquin, M.; Faraj, A.; Grandjean, J. *Oil Gas Sci. Technol.* **2014**, *69*, 865–884.
- (15) Evans, M. G.; Polanyi, M. *Trans. Faraday Soc.* **1935**, *31*, 875–894.
- (16) Frisch, M. J. et al. *Gaussian 16*, Revision C.01; Gaussian, Inc.: Wallingford, CT, 2016.
- (17) *MedeA: Materials Exploration and Design Analysis*. Copyright © 1998–2020, Version 3.1; Materials Design, Inc..
- (18) McQuarrie, D. A.; Simon, J. D. *Molecular Thermodynamics*; University Science Books: 1999.
- (19) Becke, A. D. *Phys. Rev. A: At., Mol., Opt. Phys.* **1988**, *38*, 3098–3100.
- (20) Lee, C.; Yang, W.; Parr, R. G. *Phys. Rev. B: Condens. Matter Mater. Phys.* **1988**, *37*, 785–789.
- (21) Hariharan, P. C.; Pople, J. A. *Theor. Chem. Acc.* **1973**, *28*, 213–22.
- (22) Franch, M. M.; Pietro, W. J.; Hehre, W. J.; Binkley, J. S.; DeFrees, D. J.; Pople, J. A.; Gordon, M. S. *J. Chem. Phys.* **1982**, *77*, 3654–3665.
- (23) Rassolov, V. A.; Ratner, M. A.; Pople, J. A.; Redfern, P. C.; Curtiss, L. A. *J. Comput. Chem.* **2001**, *22*, 976–984.
- (24) Marenich, A. V.; Cramer, C. J.; Truhlar, D. G. *J. Phys. Chem. B* **2009**, *113*, 6378–6396.
- (25) Rinaldi, D.; Rivail, J. L. *Theor. Chim. Acta* **1973**, *32*, 57–70.
- (26) Miertuš, S.; Scrocco, E.; Tomasi, J. *Chem. Phys.* **1981**, *55*, 117–129.
- (27) Barone, V.; Cossi, M.; Tomasi, J. *J. Comput. Chem.* **1998**, *19*, 404–417.
- (28) Klamt, A.; Schüürmann, G. *J. G. J. Chem. Soc., Perkin Trans. 2* **1993**, 799–805.
- (29) Klamt, A. *J. Phys. Chem.* **1995**, *99*, 2224–2235.
- (30) Klamt, A.; Jonas, V.; Bürger, T.; Lohrenz, J. C. *J. Phys. Chem. A* **1998**, *102*, 5074–5085.
- (31) Beglov, D.; Roux, B. *J. Phys. Chem. B* **1997**, *101*, 7821–7826.
- (32) Kovalenko, A.; Hirata, F. *J. Chem. Phys.* **1999**, *110*, 10095–10112.
- (33) Nakai, H.; Ishikawa, A. *J. Chem. Phys.* **2014**, *141*, 174106.
- (34) Cramer, C. J.; Truhlar, D. G. *Chem. Rev.* **1999**, *99*, 2161–2200.
- (35) Kamlet, M. J.; Taft, R. W. *J. Am. Chem. Soc.* **1976**, *98*, 377–383.
- (36) Taft, R. W.; Kamlet, M. J. *J. Am. Chem. Soc.* **1976**, *98*, 2886–2894.
- (37) Abraham, M. H.; Grellier, P. L.; Kamlet, M. J.; Doherty, R. M.; Taft, R. W.; Abboud, J. L. *Rev. Port. Quím.* **1989**, *31*, 85–92.
- (38) Thomson, G. H. *Int. J. Thermophys.* **1996**, *17*, 223–232.
- (39) DIPPR (Design Institute for Physical Property Datafiles), Version 17.0; American Institute of Chemical Engineers: 2019.
- (40) Emmert-Streib, F. *Statistical modelling of molecular descriptors in QSAR/QSPR*; John Wiley & Sons: 2012.
- (41) Nieto-Draghi, C.; Fayet, G.; Creton, B.; Rozanska, X.; Rotureau, P.; de Hemptinne, J. C.; Ungerer, P.; Rousseau, B.; Adamo, C. *Chem. Rev.* **2015**, *115*, 13093–13164.
- (42) Joback, K. G.; Reid, R. C. *Chem. Eng. Commun.* **1987**, *57*, 233–243.

- (43) Dumanovic, D.; Kosanovic, D. J.; Ardakovic, D.; Jovanovic, J. *Pharmazie* **1992**, *47*, 603–607.
- (44) Jouyban, A.; Soltanpour, S.; Chan, H. K. *Int. J. Pharm.* **2004**, *269*, 353–360.
- (45) Dash, S. K.; Bandyopadhyay, S. S. *Int. J. Greenhouse Gas Control* **2016**, *44*, 227–237.
- (46) Allen, M. P.; Tildesley, D. J. *Computer simulation of liquids*; Oxford University Press: 1987.
- (47) Plimpton, S. *J. Comput. Phys.* **1995**, *117*, 1–19.
- (48) Sun, H.; Mumby, S. J.; Maple, J. R.; Hagler, A. T. *J. Am. Chem. Soc.* **1994**, *116*, 2978–2987.
- (49) Yiannourakou, M.; Ungerer, P.; Leblanc, B.; Rozanska, X.; Saxe, P.; Vidal-Gilbert, S.; Gouth, F.; Montel, F. *Oil Gas Sci. Technol.* **2013**, *68*, 977–994.
- (50) Ungerer, P.; Rigby, D.; Leblanc, B.; Yiannourakou, M. *Mol. Simul.* **2014**, *40*, 115–122.
- (51) Rozanska, X.; Ungerer, P.; Leblanc, B.; Saxe, P.; Wimmer, E. *Oil Gas Sci. Technol.* **2015**, *70*, 405–417.
- (52) Luty, B. A.; Davis, M. E.; Tironi, I. G.; Van Gunsteren, W. F. *Mol. Simul.* **1994**, *14*, 11–20.
- (53) Daura, X.; Mark, A. E.; Van Gunsteren, W. F. *J. Comput. Chem.* **1998**, *19*, 535–547.
- (54) Evans, D. J.; Holian, B. L. *J. Chem. Phys.* **1985**, *83*, 4069–4074.
- (55) Frenkel, D.; Smit, B. *Understanding molecular simulation: from algorithms to applications*; Elsevier: 2001; Vol. 1, DOI: [10.1016/B978-0-12-267351-1.XS000-7](https://doi.org/10.1016/B978-0-12-267351-1.XS000-7).
- (56) Evans, M. G.; Polanyi, M. *Trans. Faraday Soc.* **1938**, *34*, 11–24.
- (57) Svelle, S.; Tuma, C.; Rozanska, X.; Kerber, T.; Sauer, J. *J. Am. Chem. Soc.* **2009**, *131*, 816–825.
- (58) Yang, X.; Rees, R. J.; Conway, W.; Puxty, G.; Yang, Q.; Winkler, D. A. *Chem. Rev.* **2017**, *117*, 9524–9593.
- (59) Sumon, K. Z.; Henni, A.; East, A. L. *Ind. Eng. Chem. Res.* **2012**, *51*, 11924–11930.
- (60) Mansouri, K.; Grulke, C. M.; Judson, R. S.; Williams, A. J. *J. Cheminf.* **2018**, *10*, 10.
- (61) Matsui, T.; Shigeta, Y.; Morihashi, K. *J. Chem. Theory Comput.* **2017**, *13*, 4791–4803.
- (62) Sakti, A. W.; Nishimura, Y.; Nakai, H. *J. Chem. Theory Comput.* **2018**, *14*, 351–356.
- (63) Skynner, R. E.; McDonagh, J. L.; Groom, C. R.; Van Mourik, T.; Mitchell, J. B. O. *Phys. Chem. Chem. Phys.* **2015**, *17*, 6174–6191.
- (64) Tomasi, J.; Mennucci, B.; Cammi, R. *Chem. Rev.* **2005**, *105*, 2999–3094.
- (65) Chea, J. D.; Lehr, A. L.; Stengel, J. P.; Savelski, M. J.; Slater, C. S.; Yenkie, K. M. *Ind. Eng. Chem. Res.* **2020**, *59*, 5931–5944.
- (66) Noroozi, J.; Smith, W. R. *J. Phys. Chem. A* **2019**, *123*, 4074–4086.
- (67) Porcheron, F.; Jacquin, M.; El Hadri, N.; Saldana, D. A.; Goulon, A.; Faraj, A. *Oil Gas Sci. Technol.* **2013**, *68*, 469–486.
- (68) Gonfa, G.; Bustam, M. A.; Shariff, A. M. *Int. J. Greenhouse Gas Control* **2016**, *49*, 372–378.
- (69) Kuenemann, M. A.; Fourches, D. *Mol. Inf.* **2017**, *36*, 1600143.
- (70) Cheng, J.; Zhu, K.; Lu, H.; Yue, H.; Liu, C.; Liang, B.; Tang, S. *Ind. Eng. Chem. Res.* **2019**, *58*, 13848–13857.
- (71) Khaheshi, S.; Riahi, S.; Mohammadi-Khanaposhtani, M.; Shokrollahzadeh, H. *Ind. Eng. Chem. Res.* **2019**, *58*, 8763–8771.
- (72) Rezaei, B.; Riahi, S.; Gorji, A. E. *Korean J. Chem. Eng.* **2020**, *37*, 72–79.
- (73) Trinh, T. T.; Rozanska, X.; Delbecq, F.; Sautet, P. *Phys. Chem. Chem. Phys.* **2012**, *14*, 3369–3380.
- (74) Roystman, V. A.; Singleton, D. A. *J. Am. Chem. Soc.* **2020**, *142*, 12865–12877.